DFT Analysis of Fe-Si Crystal Structure Stabilities

Jason M. Montgomery*
Department of Chemistry
Florida Southern College

Nidhi Choudhary†
Department of Electrical Engineering
Manipal University

Hijas KM‡
Indian Institute of Science Education and Research Thiruvananthapuram

(Dated: December 11, 2022)

Abstract: Presently electric steel with 1 - 3 wt% Si is used worldwide in electromagnetic devices, such as motors, generators, and transformers. Electric steel with 6.5 wt% Si is desirable to increase efficiency and reduces energy losses, but due to its brittleness, the material cannot be processed to the necessary thickness using conventional methods. In this paper, we describe thermodynamic stability studies of various Fe-Si alloys with 6.7 wt% Si, namely $Fe_{14}Si_2$ (16 atom unit cell) and $Fe_{28}Si_4$ (32 atom unit cell), using plane-wave density functional theory in an attempt to find stable geometries (relative to bcc-Fe and DO3-Fe_3Si) that increase Si - Si atom pair separations within the unit cell. All $Fe_{14}Si_2$ structures were found to be metastable compared to the stable $Fe_{28}Si_4$ structure, whose formation energy was found to be only 0.001 eV/atom above the convex hull phase diagram between bcc-Fe and DO3-Fe_3Si.

I. INTRODUCTION

The term "electric steel" refers to soft magnetic Fe-Si alloys, with wt% Si ranging from 0 wt% Si (bcc-Fe) to 6.5 wt% Si (Fe_5Si), that exhibit desirable magnetic properties for applications in electric motors, generators, and transformers.[1] Electric steel for commercial applications is processed by pressing strips of the metal through rollers at room temperature to reduce the thickness to 2 mm or less. However, above 3.2 wt% Si, the metal becomes too brittle for this cold-rolling process, and additional thermomechanical processes are required in order to overcome its brittleness and limited ductility.[2] The brittleness is believed to derive from short-range order of the Si atoms in the unit cell, which then extends to long range order over the crystal.

The aim of this project is to explore the thermodynamic stability of electric steel with varying concentrations of wt% Si and varying unit cell geometries using density functional theory in an attempt to find new stable, ordered structures close to 6.5 wt% Si. While no direct attempt is made to assess the brittleness of these new alloys, an additional aim is to find stable structures that increase the lattice parameter of the unit cell, thereby increasing the distance between Si atoms and reducing, to some extent, short range order. Thermodynamic stability is measured relative to two limiting compositions, elemental bcc-Fe (0 wt% Si) and DO3-Fe_3Si (14.4 wt% Si). Energies of formation are illustrated using a convex hull phase diagram approach,[3] in which calculated energies per atom of the Fe-Si alloys are compared to the line connecting bcc-Fe and DO3-Fe_3Si energies per atom. Positive deviations from this line correspond to unstable materials that would spontaneously decompose into bcc-Fe and DO3-Fe_3Si.

II. METHODS

Simulations for a range of Fe-Si alloys, ranging from bcc-Fe to DO3-Fe_3Si, were performed using plane-wave density functional theory, as implemented in the Quantum ESPRESSO (QE) package.[4] The PBE exchange-correlation

* jmontgomery@flsouthern.edu
† nidhi19jun@gmail.com
‡ hijaskm@iisertvm.ac.in

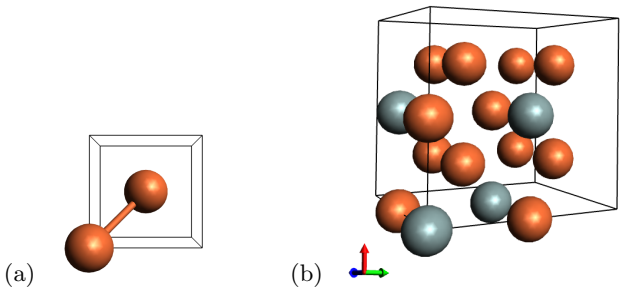

FIG. II.1. (a) bcc-Fe unit cell with $A = 2.8401$Å. (b) DO3-Fe_3Si unit cell with $A = 5.602564$ Å.

functional was used with PAW pseudopotentials downloaded from the SSSP precision library.[5] For bcc-Fe and DO3-Fe_3Si, QE input scripts were generated using *Materials Cloud*'s QE Generator tool[6] based on cif files downloaded from the *Materials Project*. The corresponding bcc-Fe unit cell contains two Fe atoms with a lattice parameter of $A = 2.8401$ Å (see Fig. II.1 (a)). The DO3-Fe_3Si unit cell contains twelve Fe atoms and four Si atoms with a lattice parameter of $A = 5.602564$ Å (see Fig. II.1 (b)). A convergence study was performed in which crystal energies (E (Ry)) for bcc-Fe and DO3-Fe_3Si were calculated with respect to k-mesh size and kinetic energy cutoffs for wavefunctions (*ecutwfc*) and charge density (*ecutrho*). Energies were considered converged with respect to k-mesh and basis set when the change in energy for successive calculations was less than 0.001 Ry. Results are described in Sec. III A.

Geometry optimizations were also performed for bcc-Fe and DO3-Fe_3Si. Static SCF calculations were first performed for a range of lattice parameters about $A = 2.8401$ Å for Fe and a range of lattice parameters about $A = 5.602564$ Å for DO3-Fe_3Si. Subsequent variable cell relaxation calculations were performed for each lattice parameter within the range at applied pressures derived from the static SCF results. The resulting energies and volumes were fit to the Birch-Murnaghan equation of state (EOS)[7] as implemented in QE's ev.x program to find the minimum energy (E_0), volume (V_0), and bulk modulus (B_0). Results are discussed in Sec. III B. Geometry optimizations were also performed for Fe-Si alloys with Si concentrations between that of bcc-Fe and DO3-Fe_3Si. Structures i - iii contain one, two, and three Si atoms, respectively, substituted with Fe atoms (Fig. IV.1). Structure ii has a 6.7 wt%Si concentration, close to the desired 6.5 wt%Si. A total of four unique structures (iia) - (iid) contain two Si atoms at different distances. (Fig. **??**). Static SCF calculations were run for each structure about a range of lattice parameters about $A = 5.602564$ Å followed by vc-relax calculations and a fit to the Birch-Murnaghan EOS to find the minimum energy (E_0), volume (V_0), and bulk modulus (B_0). Finally, a geometry optimization was also performed for a structure (iv) composed of a $2 \times 1 \times 1$ supercell of the DO3-Fe_3Si structure with four Si atoms relaced with Fe, giving rise to another 6.7 wt%Si structure but with an increased distance between Si pairs (Fig. IV.3).

Based on E_0 values for bcc-Fe and DO3-Fe_3Si, a convex hull connecting bcc-Fe and DO3-Fe_3Si was constructed, given by the equation of the line connecting $E_{\mathrm{bcc-Fe}}$ (eV/atom) and $E_{\mathrm{DO3-Fe_3Si}}$ (eV/atom):

$$E_{\mathrm{hull}}(\mathrm{eV/atom}) = 38.41360188 \times (\mathrm{at\%\ Si}) - 4478.102736 \tag{II.1}$$

The energy difference between the calculated optimized energy per atom of an Fe-Si alloy and the hull is a measure of the alloy's thermodynamic stability, or lackthereof:

$$\Delta E = E_{\mathrm{calc}} - E_{\mathrm{hull}} \tag{II.2}$$

A positive ΔE corresponds to a thermodynamically unstable alloy that would decompose into bcc-Fe and DO3-Fe_3Si. Geometry optimization and stability results for structures (i) - (iv) are discussed in Sec. IV.

III. RESULTS

A. Convergence Results for bcc-Fe and DO3-Fe_3Si

A series of static SCF calculations were performed for both bcc-Fe and DO3-Fe_3Si to determine the k-mesh size and basis-set size required for energies to be converged to better than 0.001 Ry. To determine the k-mesh size, the basis set size was fixed with *ecutwfc* = 90.0 Ry and *ecutrho* = 1080.0 Ry for increasing K_POINTS. To determine

convergence with respect to basis-set, *ecutwfc* was increased while keeping *ecutrho* = 12×*ecutwfc*. Convergence with respect to *ecutrho* was determined by setting *ecutrho* = $f\times$ *ecutwfc* and varying the factor f. Results are listed in Tables I, Table II, and III, respectively. Entries in bold-font represent the minimum value of each parameter required to converge energies for both bcc-Fe and DO3-Fe_3Si simultaneously, namely $9\times9\times9$ k-mesh with *ecutwfc* = 140.0 Ry and *ecutrho* = 840.0 Ry. While the hydrostatic pressure is not yet converged at $9\times9\times9$ k-mesh for Fe, the energy is converged to better than 0.0002 Ry compared to the $19\times19\times19$ k-mesh. Given that stability is a function of energy, and given we will be using lattice parameters on the order of DO3-Fe_3Si for the 6.25%wtSi, the $9\times9\times9$ k-mesh will suffice.

TABLE I. Convergence based on k-mesh

crystal	k-points	# k-points	Energy (Ry)	ΔE (Ry)	P (kbar)
bcc-Fe	1,1,1	1	-658.9316114		-21.62
	3,3,3	4	-658.5588004	0.37281096	-16.43
	5,5,5	10	-658.5456948	0.0131056	-29.34
	7,7,7	20	-658.5433615	0.00233331	-13.61
	9,9,9	35	-658.5432048	0.00015667	-18.05
	11,11,11	56	-658.5430047	0.00020012	-13.47
	13,13,13	84	-658.5430670	-6.229E-05	-16.02
	15,15,15	120	-658.5429717	9.528E-05	-15.61
	17,17,17	165	-658.5430197	-4.798E-05	-16.60
	19,19,19	220	-658.543059	-3.927E-05	-15.63
DO3-Fe_3Si	3,3,3	4	-4138.533134		0.29
	5,5,5	10	-4138.536424	-0.0032908	1.29
	7,7,7	20	-4138.536466	-4.131E-05	3.99

[1] ecutwfc = 90.d0 Ry, ecutrho = 1080.d0 Ry

TABLE II. Convergence based on ecutwfc

crystal	ecutwfc (Ry)	Energy (Ry)	ΔE(Ry)	P (kbar)
bcc-Fe	70	-658.5427068		-45.64
	80	-658.5456495	-0.00595909	-32.45
	90	-658.5442528	-0.00190518	-18.05
	100	-658.5434732	-0.00022592	-15.57
DO3-Fe_3Si	70	-4138.489585		-18.31
	80	-4138.524986	-0.03540055	-7.75
	90	-4138.536466	-0.0114798	3.99
	100	-4138.537799	-0.00133387	5.7
	110	-4138.539696	-0.00189652	3.85
	120	-4138.542673	-0.00297671	3.41
	130	-4138.544834	-0.00216137	4.49
	140	-4138.545738	-0.00090385	5.56

[1] Fe: k-mesh = $9\times9\times9$; Si: k-mesh = $7\times7\times7$, *ecutrho* = 12×*ecutwfc*

TABLE III. Convergence based on ecutrho

crystal	ecutrho (Ry)	Energy (Ry)	Δ E (Ry)	P (kbar)
bcc-Fe	400	-658.5436683		-13.95
	500	-658.5438748	-0.00020653	-13.46
	600	-658.5434504	0.00042437	-15.35
	700	-658.5435172	-6.676E-05	-15.69
DO3-Fe_3Si	700	-4138.5462		5.62
	840	-4138.545784	0.00041543	5.68
	1120	-4138.545758	2.601E-05	5.64

[1] Fe: k-mesh = $9\times9\times9$, ecutwfc = 100. Ry
[2] Si: k-mesh = $7\times7\times7$, ecutwfc = 140. Ry

B. Geometry Optimization Results for bcc-Fe and DO3-Fe_3Si.

Geometry optimization calculations were performed by first calculating static SCF energies and pressures for a range of lattice parameters. Table IV lists the lattice parameters, volumes, energies, and corresponding hydrostatic pressures for both bcc-Fe and DO3-Fe_3Si. Variable-cell relaxation (vc-relax) calculations were then performed subject to corresponding applied pressures to find the optimal unit cell geometry and atomic coordinates at each pressure. No change in geometry or energy was observed for any of the vc-relax calculations for either crystal. A fit to the Birch-Murnaghan equation of states (EOS) was used to determine the optimal cell volume, energy, and bulk modulus, which are also listed in Table IV. As a test, SCF calculations were run at the predicted V_0 for each crystal. For bcc-Fe, P = 1.50 kbar and E = -658.54482475 Ry, and for DO3-Fe_3Si, P = 0.88 kbar and E = -4138.54543564 Ry, very close to the expected zero hydrostatic pressure and in good agreement with the E_0 values predicted from the Birch-Murnaghan EOS.

TABLE IV. Variable cell relaxation calculation results and resulting EOS parameters for bcc-Fe and DO3-Fe_3Si.

crystal[1]	A (Å)	V (Å^3)	E (Ry)	P (kbar)	EOS
bcc-Fe	2.76005168	21.0257571	-658.53734	194.33	$E_{\mathrm{bcc-Fe}} = -658.54452$ Ry
	2.80005168	21.9532155	-658.54329	85.14	(-329.27226 eV/atom)
	2.84005168	22.9075545	-658.54477	-15.8	$V_0 = 22.73$ Å^3
	2.88005168	23.889158	-658.54223	-90.03	$A_0 = 2.83269$ Å
	2.92005168	24.89841	-658.53711	-126.38	$B_0 = 190.9$ GPa
	2.96005168	25.9356944	-658.53067	-142.7	
DO3-Fe_3Si	5.409216069	158.2715984	-4138.476005	283.67	$E_{\mathrm{Fe3Si}} = -4138.54434$ Ry
	5.50758694	167.064465	-4138.527521	127.56	(-258.65909 eV/atom)
	5.602564	175.8573316	-4138.545361	6.06	$V_0 = 176.27$ Å^3
	5.694425638	184.6501982	-4138.519708	-93.15	$A_0 = 5.60694$ Å
	5.783415413	193.4430647	-4138.438115	-147.67	$B_0 = 216.3$ GPa

[1] The vc-relax calculations gave no change in volume or geometry for both crystals.

IV. THE GRAND SEARCH

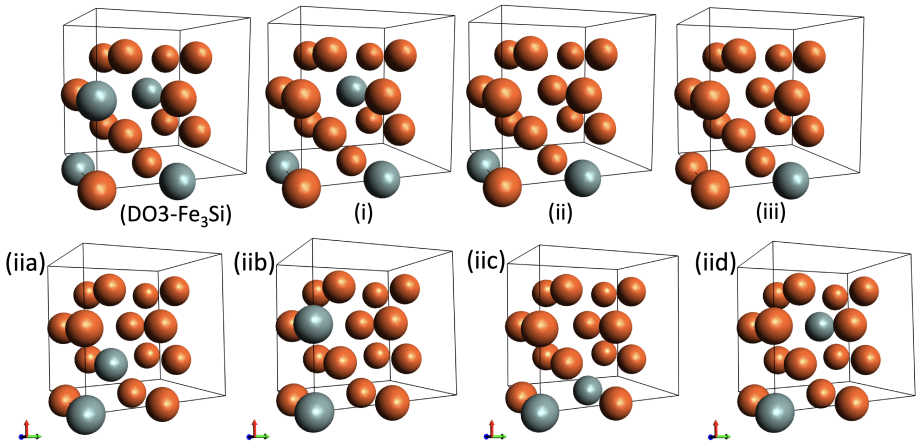

FIG. IV.1. Unit-cells for DO3-Fe_3Si(25 at%Si, 14.4 wt%Si), structure (i) ($Fe_{13}Si_3$, 18.75 at%Si, 10.4 wt%Si), (ii) ($Fe_{14}Si_2$, 12.5 at%Si, 6.7 wt%Si), (iii) ($Fe_{15}Si$, 6.5 at%Si, 3.2 wt%Si). Unit-cells for structure ii with varying Si atoms replaced with Fe, giving rise to different Si-Si distances: (iia) 2.426Å, (iib) 2.801Å, (iic) 3.962Å, (iid) 4.852Å

Figure IV.1 contains images of unit cells for Fe-Si alloys with wt% Si compositions between that of bcc-Fe and DO3-Fe_3Si. Structures (i - iii) each have sixteen atoms in the unit cell in which Si atoms in DO3-Fe_3Si are replaced

with a corresponding number of Fe atoms – (i) ($Fe_{13}Si_3$, 18.75 at%Si, 10.40 wt% Si), (ii) ($Fe_{14}Si_2$, 12.5 at%Si, 6.70 wt% Si), and (iii) ($Fe_{15}Si$, 6.25 at%Si, 3.24 wt% Si). While not in the wt% Si range of interest, structures (i) and (iii) were included in order to see how the substitution of increasing numbers of Si atoms with Fe affected stability. Structure (ii) has a Si composition close to the desired 6.5 wt% Si. Therefore, a total of 4 structures (iia) - (iid) were studied. Each differs in the distance between Si atoms in the unit cell, namely 2.426 Å, 2.801 Å, 3.962 Å, and 4.852 Å, respectively. Structure (iic), whose Si - Si distance is closest to that in DO3-Fe_3Si, gave rise to the lowest minimum energy geometry (Fig. IV.2).

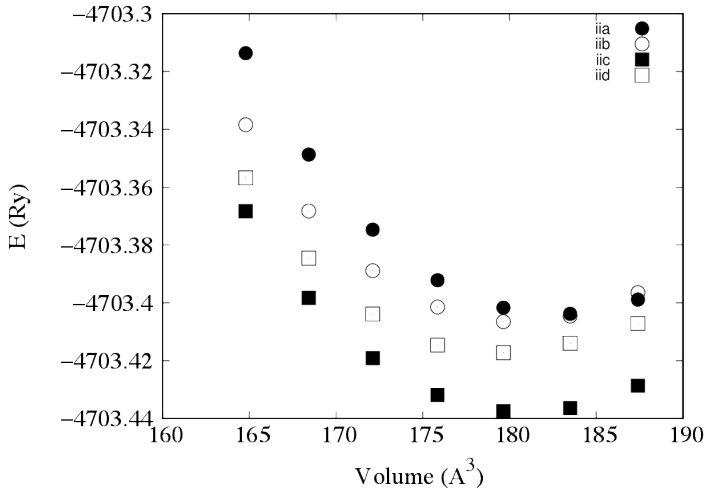

FIG. IV.2. ΔE Structure ii calculated Energy (Ry) vs Volume for different positions of Si

Table V contains the results of geometry optimizations and stability analysis for structures (i), (iic), and (iii). Structures (i) and (iii) were found to be $\Delta E < 0.01$ eV/atom above the hull (Eqn. II.1). Structure (iic) was less stable with $\Delta E = 0.011$ eV/atom.

A tetragonal crystal unit cell also with 6.7 wt% Si, structure (iv) (Fig. IV.3), was also constructed by replacing the interior Si atoms of a 2×1×1 supercell of DO3-Fe_3Si. The aim of this structure was increase the stability by increasing the average distance between Si-Si atom pairs, and it was found to be an order of magnitude more stable with $\Delta E = 0.001$ eV/atom, essentially on the hull. ΔE values for all structures are depicted in Fig. IV.4. To put these ΔE values in perspective, Materials Project lists ΔE values on the order of 0.01 to 0.21 for a range of higher Si compositions.

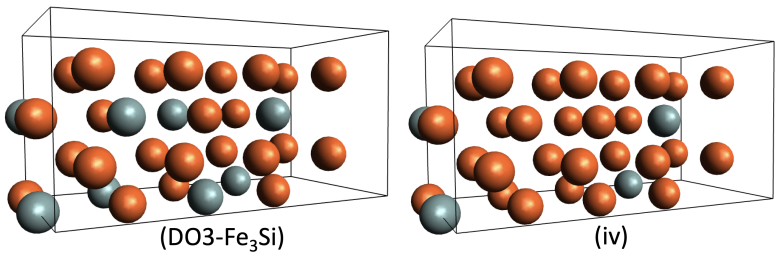

FIG. IV.3. Unit-cells for structure ii with varying Si atoms replaced with Fe, giving rise to different Si-Si distances: (iia) 2.426Å, (iib) 2.801Å, (iic) 3.962Å, (iid) 4.852Å

TABLE V. Replacing Si atoms in DO3-Fe_3Si and 2×1×1 supercell

	structure (i)	structure (iic)	structure (iii)	structure (iv)
Fe atoms	13	14	15	28
Si atoms	3	2	1	4
at% Si	18.75	12.5	6.25	12.5
wt% Si	10.40	6.70	3.24	6.70
V_0 Å^3	178.38	182.68	181.53	360.08
B_0 GPa	194.2	177.9	174.0	189.9
E_0 (Ry/cell)	-4420.987	-4703.438	-4985.897	-9406.898
E_0 (eV/atom)	-3757.839	-3997.922	-4238.012	-3997.932
E_{hull} (eV/atom)	-3997.933	-3997.933	-4238.018	-3997.933
ΔE (eV/atom)	0.009	0.011	0.006	0.001

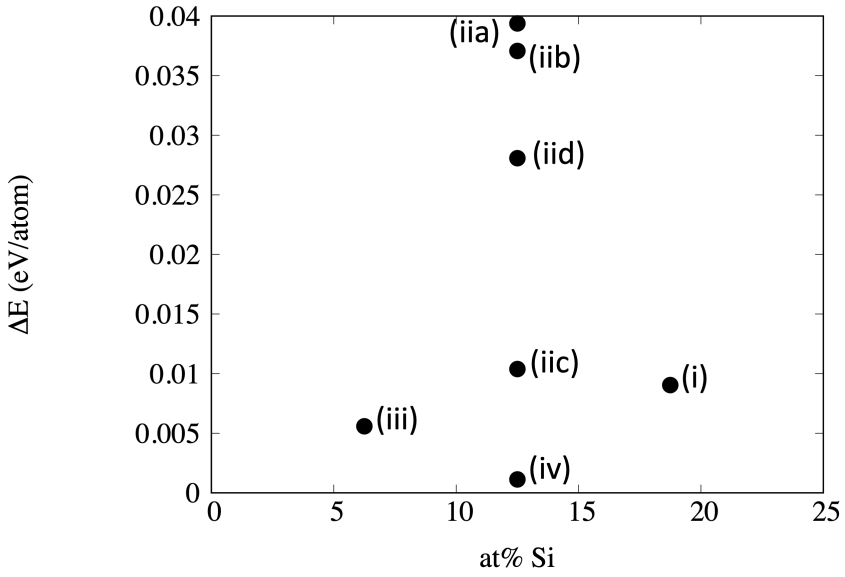

FIG. IV.4. ΔE values for structure (i) - (iv).

V. CONCLUSION

Ab initio calculations were performed using plane-wave density functional theory and Quantum Espresso package to check the stability of a total of seven Fe-Si alloys with Si compositions ranging from 3.2 to 10.4 wt% Si. An emphasis was placed on alloys with a 6.7 wt% Si composition, for which a 16-atom cubic unit cell (structure (iic), $A = 5.662$ Å) was found to lie 0.011 eV/atom above the convex hull phase diagram and a tetragonal 32-atom unit cell (structure (iv), $A = 11.293$, $B = C = 5.647$ Å) was found to lie 0.001 eV/atom. The increase in stability of the tetragonal structure accompanies an increase in the average distance between Si-Si atom pairs. Future work will focus on the stability larger tetragonal or cubic unit cells and the corresponding elasticity of these alloys.

VI. ACKNOWLEDGEMENT

We would like to thank Prof. Stefaan Cottenier of Ghent University for his time and effort in creating and administering the online course in DFT and Quantum Espresso and for his helpful discussions throughout this project.

VII. REFERENCES

[1] G. Ouyang, X. Chen, Y. Liang, C. Macziewski, and J. Cui, Journal of Magnetism and Magnetic Materials **481**, 10.1016/j.jmmm.2019.02.089 (2019).

[2] T. Ros-Yañez, Y. Houbaert, O. Fischer, and J. Schneider, Production of high silicon steel for electrical applications by thermomechanical processing, Journal of Materials Processing Technology **143-144**, 916 (2003), proceedings of the International Conference on the Advanced Materials Processing Technology, 2001.

[3] A. Van Alboom, B. Lemmens, B. Breitbach, E. De Grave, S. Cottenier, and K. Verbeken, Multi-method identification and characterization of the intermetallic surface layers of hot-dip al-coated steel: Feal3 or fe4al13 and fe2al5 or fe2al5+x, Surface and Coatings Technology **324**, 419 (2017).

[4] P. Giannozzi, S. Baroni, N. Bonini, M. Calandra, R. Car, C. Cavazzoni, D. Ceresoli, G. L. Chiarotti, M. Cococcioni, I. Dabo, A. D. Corso, S. de Gironcoli, S. Fabris, G. Fratesi, R. Gebauer, U. Gerstmann, C. Gougoussis, A. Kokalj, M. Lazzeri, L. Martin-Samos, N. Marzari, F. Mauri, R. Mazzarello, S. Paolini, A. Pasquarello, L. Paulatto, C. Sbraccia, S. Scandolo, G. Sclauzero, A. P. Seitsonen, A. Smogunov, P. Umari, and R. M. Wentzcovitch, Quantum espresso: a modular and open-source software project for quantum simulations of materials, Journal of Physics: Condensed Matter **21**, 395502 (2009).

[5] J. P. Perdew, K. Burke, and Y. Wang, Generalized gradient approximation for the exchange-correlation hole of a many-electron system, Phys. Rev. B **54**, 16533 (1996).

[6] L. Talirz, S. Kumbhar, E. Passaro, A. V. Yakutovich, V. Granata, F. Gargiulo, M. Borelli, M. Uhrin, S. P. Huber, S. Zoupanos, C. S. Adorf, C. W. Andersen, O. Schütt, C. A. Pignedoli, D. Passerone, J. VandeVondele, T. C. Schulthess, B. Smit, G. Pizzi, and N. Marzari, Materials cloud, a platform for open computational science, Scientific Data **7**, 10.1038/s41597-020-00637-5 (2020).

[7] F. Birch, Finite Elastic Strain of Cubic Crystals, Physical Review **71**, 809 (1947).